Glass Forming Ability of La-rich La–Al–Cu Ternary Alloys

Hao Tan[1], Zhaoping Lu[1], Haibiao Yao[1], Bin Yao[1], Yuanping Feng[2] and Yi Li[1, *]

[1] *Department of Materials Science, Faculty of Science, National University of Singapore, 119260, Singapore*

[2] *Department of Physics, Faculty of Science, National University of Singapore, 119260, Singapore*

Melting behavior and the reduced glass transition temperature (T_{rg}) in La-rich La–Cu–Al based alloys was systematically investigated. It was found that reduced glass transition temperature increased to the maximum when the liquidus temperature decreased to the minimum for La$_{86-x}$Cu$_x$Al$_{14}$ ($x = 10$–36) alloys. The best glass formation in La-rich La–Cu–Al ternary system was obtained at La$_{66}$Cu$_{20}$Al$_{14}$ alloy, which is at a eutectic point with the highest reduced glass transition temperature of 0.541 among these alloys. The glass forming ability of these alloys is correlated and discussed with their reduced glass transition temperature.

1. Introduction

Since the late 1980s, bulk glass formation has been reported in various new alloy systems. For example, 9 and 5 mm diameter glassy rods were obtained in La$_{55}$Al$_{25}$Ni$_{10}$Cu$_5$Co$_5$ and La$_{55}$Al$_{25}$Ni$_{10}$Cu$_{10}$.[1] Besides, the best glass forming alloys were either at or around a eutectic point.[2,3] However, despite the fact that La$_{55}$Al$_{25}$Cu$_{20}$ is a bulk glass forming alloy,[4] it is evidently not near a eutectic.[3] This could be an indication that even larger thickness of bulk metallic glasses may be obtained in this alloy system.

Glass forming ability (GFA) can be represented by many parameters.[5] The reduced glass transition temperature, T_{rg} defined below is one of the widely used indicators of GFA of alloys:

$$T_{rg} = \frac{T_g}{T_l} \qquad (1)$$

where T_g is the glass transition temperature and T_l is the liquidus temperature. It is believed that T_g generally has a weak dependence on composition while T_l often changes strongly with the composition.[6,7] It can be seen that if a eutectic composition could be found, there should be a maximum value for T_{rg} at this composition.

The present work was mainly undertaken to study the glass formation and glass forming ability in La$_{86-x}$Al$_{14}$Cu$_x$ ($x = $ 10 to 36) alloys. In addition, the GFA of these alloys is correlated and discussed with their reduced glass transition temperature (T_{rg}).

2. Experimental Procedure

All the alloys were prepared by arc-melting a mixture of 99.9% pure La and Al, and 99.999% pure Cu. Pieces of resulting ingots were sealed in quartz tubings with external diameter of 3 mm, which were evacuated and then back-filled with argon to minimize the oxidation during melting process. The onset melting temperature T_m and the offset temperature T_l (equivalent to liquidus temperature) of these al-

loys were obtained through the melting behavior study carried out on a differential thermal analysis (DTA) system at a heating rate of 20 K/min. Glass formation was obtained either by melt-spinning using a single roller melt-spinner under an argon atmosphere or by lower pressure chill casting into a ϕ2 mm × 30 mm long cavity of a copper mold. The glass transition temperature T_g and crystallization temperature T_x were measured with a differential scanning calorimeter (DSC) at the same heating rate of 20 K/min. Bridgman solidification through a temperature gradient of 15 K/mm was used to determine the critical cooling rate.

3. Results

3.1 Melting study

Figure 1 shows the alloy compositions in this work. DTA traces of the La$_{55}$Al$_{45-x}$Cu$_x$ alloys are shown in Fig. 2(a). It can be clearly seen that the temperature difference between T_m and T_l is very large, indicating that this alloy is away from
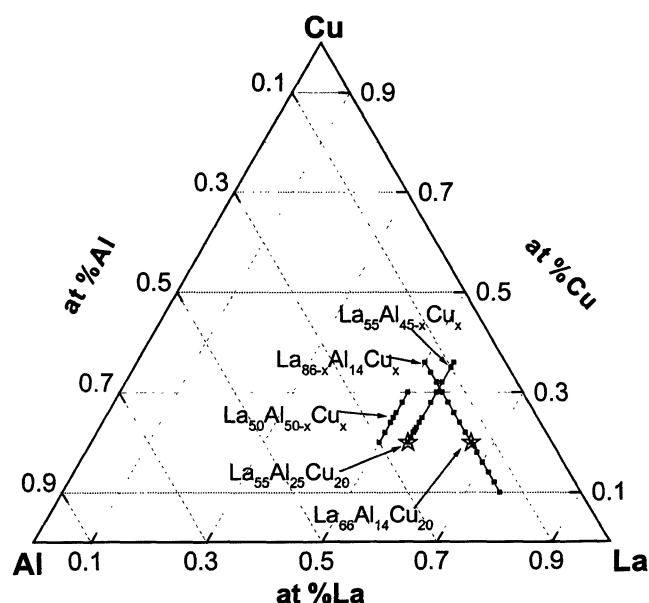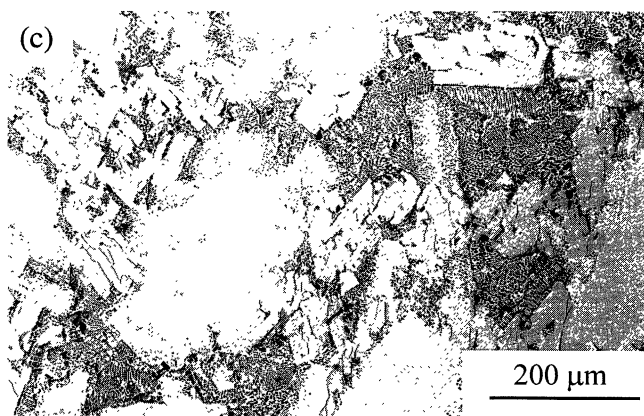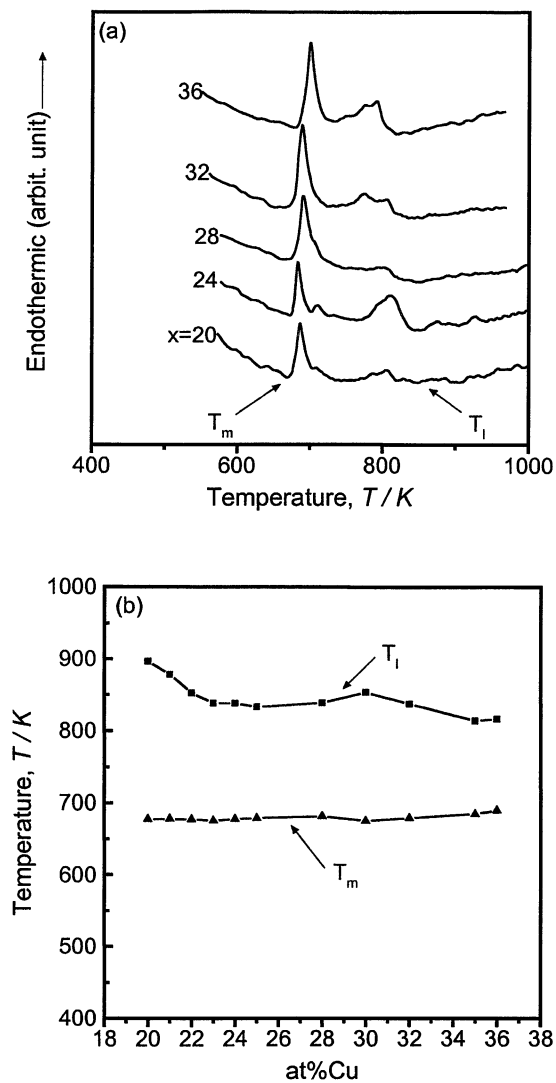

Fig. 1 Distribution of the alloys in this work.

Fig. 2 (a) DTA traces of La$_{55}$Al$_{45-x}$Cu$_x$ alloys, (b) T_m and T_l as a function of copper content for La$_{55}$Al$_{45-x}$Cu$_x$ alloys and (c) Microstructure of La$_{55}$Al$_{25}$Cu$_{20}$.

Fig. 3 (a) DTA traces of La$_{50}$Al$_{50-x}$Cu$_x$ alloys, (b) T_m and T_l as a function of copper content for La$_{50}$Al$_{50-x}$Cu$_x$ alloys and (c) Microstructure of La$_{50}$Al$_{26}$Cu$_{24}$.

eutectic point. There are at least 2 melting peaks in every trace in Fig. 2(a), which indicates that these alloys are away from eutectic composition. Values of T_m and T_l obtained from these traces are plotted as a function of copper content in Fig. 2(b). Typical microstructure for La$_{55}$Al$_{25}$Cu$_{20}$ is shown in Fig. 2(c), which can be classified as a coarse primary and a
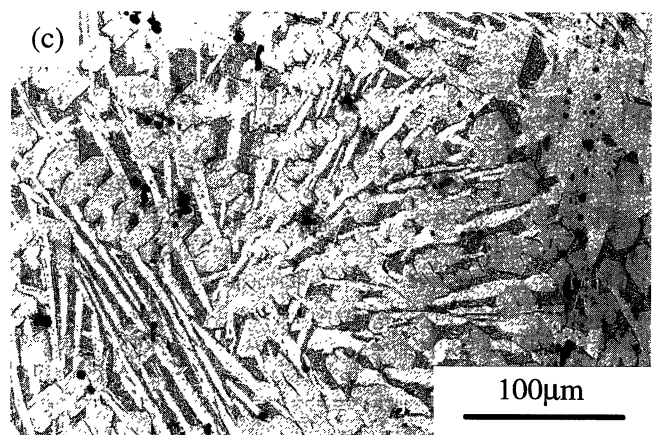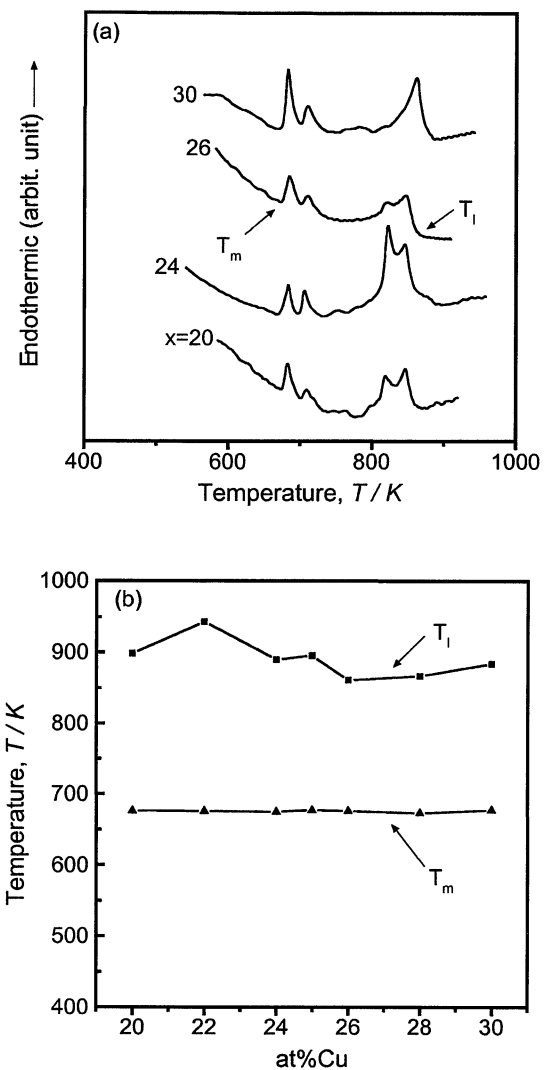
small amount of eutectic.

Figure 3(a) shows the DTA traces of the La$_{50}$Al$_{50-x}$Cu$_x$ alloys. Values of T_m and T_l are illustrated in Fig. 3(b) as a function of copper content. There are also several melting peaks in each DTA trace and the temperature difference between T_m and T_l remains around 200 K throughout the con-
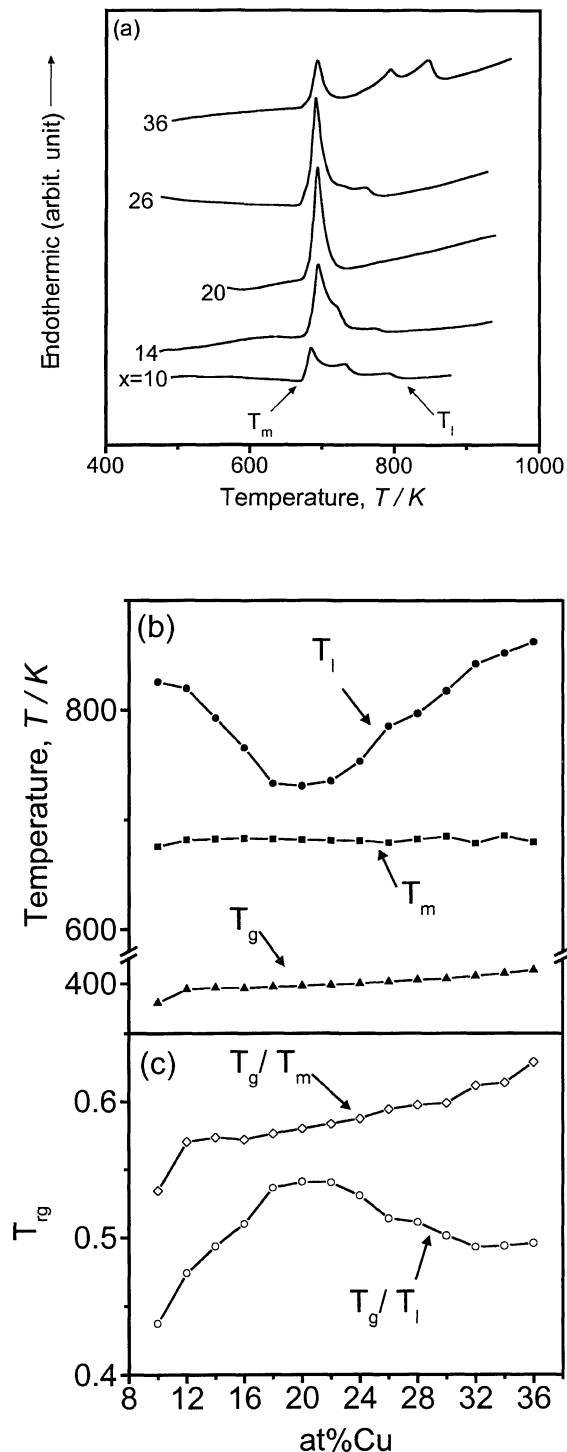
Fig. 4 (a) DTA traces of $La_{86-x}Al_{14}Cu_x$ alloys, (b) T_m and T_l as a function of copper content for $La_{86-x}Al_{14}Cu_x$ alloys and (c) T_{rg} as a function of copper content for $La_{86-x}Al_{14}Cu_x$ alloys.

Fig. 5 Microstructure of (a) $La_{68}Al_{14}Cu_{18}$, (b) $La_{66}Al_{14}Cu_{20}$ and (c) $La_{64}Al_{14}Cu_{22}$.

tent change. Figure 3(c) summarizes the microstructure of the $La_{50}Al_{26}Cu_{24}$ alloy. It can be found that the microstructure contains two kinds of primary phases (white strip-like phase and grey block-like phase) with small amount of eutectic. The large amount of these primary phases should be responsible for the high values of T_l for the $La_{50}Al_{50-x}Cu_x$ alloys.

Instead of fixing La content in the above two alloy systems, we attempted to change the La content in the alloys. DTA

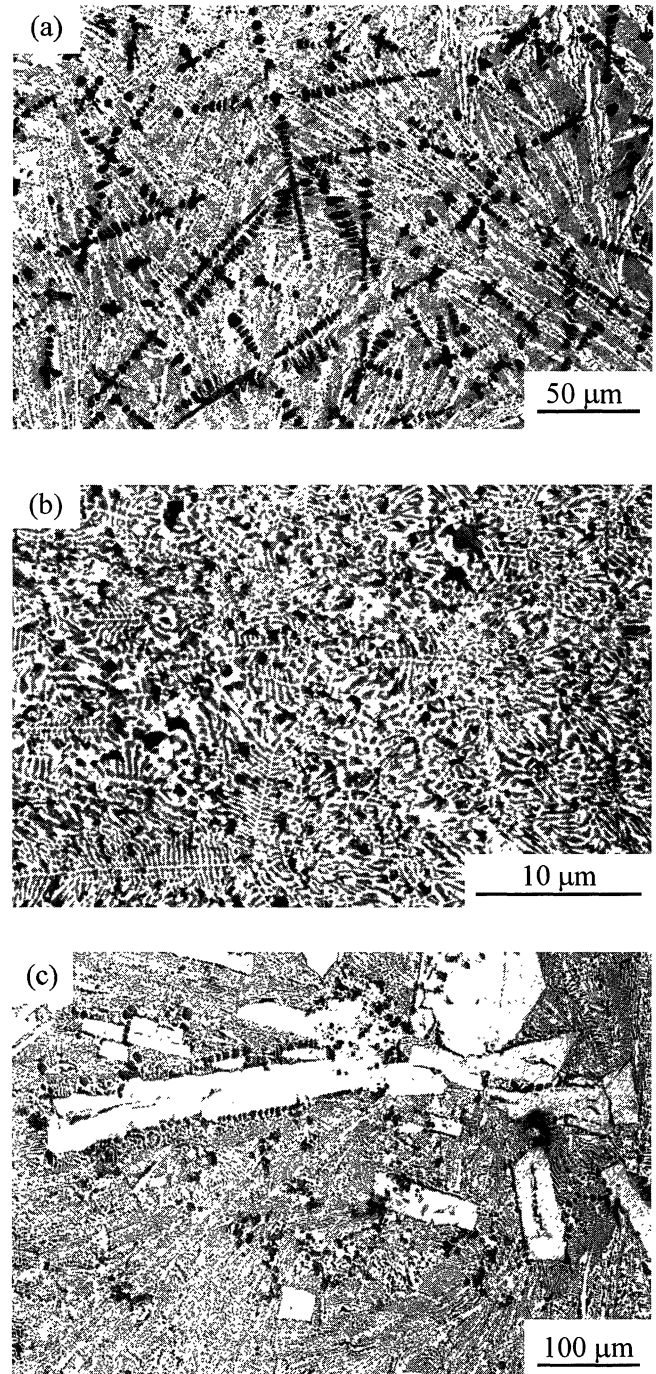traces of the $La_{86-x}Al_{14}Cu_x$ alloys are showed in Fig. 4(a). DTA traces for $La_{72}Al_{14}Cu_{14}$ and $La_{60}Al_{14}Cu_{26}$ exhibit a sharp initial melting at T_m, followed by a wide melting interval. However, the trace for $La_{66}Al_{14}Cu_{20}$ only illustrates a single large melting peak initiated at T_m. Values of T_m and T_l as a function of Cu content are plotted in Fig. 4(b), along with their T_g values. As shown in Fig. 4(b), when the Cu content increases from 10 to 20 at%, there is a sharp decrease in T_l. However, further increase in copper Cu content causes T_l goes upwards again. At the same time, T_m remains horizontal throughout the changes in concentration, which suggests there could be a eutectic reaction among all these alloys at a

temperature of 675 K.

As the composition changes, T_g, however, does not vary much. As shown in Fig. 4(b), there is only a small and gradual increase in T_g from 361 to 428 K as the Cu content increases from 10 to 36 at%, which shows that T_g of these alloys is indeed less dependent on composition than T_l.

Figures 5(a) to (c) summarizes the typical microstructure of the La68Al14Cu18, La66Al14Cu20 and La64Al14Cu22 alloys. Figure 5(b) showed clearly a fully eutectic morphology without primary phases. Although the microstructure can be classified as a primary phase plus eutectic for Figs. 5(a) and (c), the morphology of the primary phase in La68Al14Cu18 is different from that of La64Al14Cu22. These results indicate that the La66Al14Cu20 is at a eutectic point.

3.2 Glass forming ability

3.2.1 Chill casting

The characteristic temperature T_g, T_x and the heat of crystallization for the melt-spun ribbons together with the values for their corresponding chill casting rod samples of 2 mm in diameter are given in Table 1. Values of $\%\Delta H_x$ ($\Delta H_x/\Delta H_r$), which is the ratio between the enthalpy of crystallization ΔH_x for chill casting rods and that of ΔH_r for as-spun ribbons, can be regarded as the amount of single amorphous phase in the cast sample. It can be clearly seen from this table that the La66Al14Cu20 can obtain a fully glassy rod ($\%\Delta H_x = 98\%$), while the values of $\%\Delta H_x$ for other alloys are below 90% indicating that they are partially amorphous with modest bulk glass forming ability. Therefore, the La66Al14Cu20 alloy should have a high glass forming ability with a rather low value of critical cooling rate.

3.2.2 Bridgman solidification for La66Al14Cu20

Figure 6 is the $\%\Delta H_x$ for La66Al14Cu20 samples obtained from different withdraw velocities. It can be concluded from this figure that the critical growth velocity for La66Al14Cu20 should be around 2.5 mm/s. Therefore, the corresponding critical cooling rate for this alloy is 37.5 K/s (2.5 mm/s × 15 K/mm).
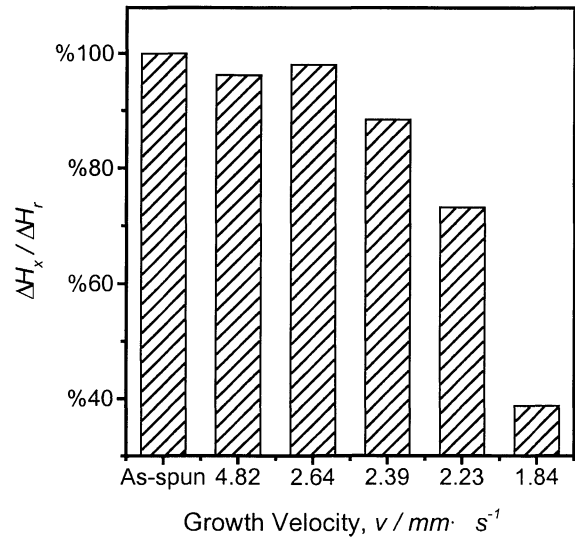

Fig. 6 $\%\Delta H_x$ of Bridgman samples for La66Al14Cu20 with different withdraw velocity.

4. Discussion

4.1 Eutectic composition and glass forming ability

Lu *et al.* have reported that the bulk glass forming alloys are those having eutectic composition or being very near to a eutectic composition.[2,3] The current study showed that the La66Al14Cu20 alloy is at a eutectic point. Chill casting result also shows that only La66Al14Cu20 can form 2 mm fully glassy rod ($\%\Delta H_x/\Delta H_r = 98\%$). Besides, the Bridgman solidification results for La66Al14Cu20 also showed that these alloy has a rather lower value of critical cooling rate than that of La55Al25Cu20,[7] which is greater than 72.3 K/s. Therefore, it can be clearly seen that the eutectic alloy in La86−xAl14Cux ($x = 10$ to 36) alloys has the greatest glass forming ability (GFA) in La–Al–Cu alloys studied so far.

Table 1   Results of DSC analysis for chill casting and as-spun samples.

Alloy name	Sample	T_g (K)	T_x (K)	$(T_x - T_g)$ (K)	ΔH_x (J/g)	$\%\Delta H_x$
La68Al14Cu18	Ribbon	393	436	43	30.9	0.68
	Casting rod	394	437	43	21.0	
La66Al14Cu20	Ribbon	395	449	54	37.4	0.98
	Casting rod	395	453	58	36.6	
La64Al14Cu22	Ribbon	398	459	61	39.8	0.90
	Casting rod	398	459	61	35.8	
La62Al14Cu24	Ribbon	400	457	57	41.7	0.81
	Casting rod	402	458	56	33.7	
La70Al14Cu26	Ribbon	404	452	48	40.8	0.90
	Casting rod	404	454	50	36.7	
La72Al14Cu28	Ribbon	408	451	43	34.3	0.85
	Casting rod	407	451	44	29.3	

Table 2   Values for characteristic temperatures (T_g, T_m and T_l) and T_{rg}.

Alloy	T_g (K)	T_m (K)	T_l (K)	T_g/T_m	T_g/T_l
$La_{50}Al_{14}Cu_{36}$	428	680.9	862.7	0.629	0.496
$La_{52}Al_{14}Cu_{34}$	421	686.0	852.3	0.614	0.494
$La_{54}Al_{14}Cu_{32}$	416	679.2	542.4	0.612	0.493
$La_{56}Al_{14}Cu_{30}$	410	685.1	817.9	0.599	0.502
$La_{58}Al_{14}Cu_{28}$	408	682.6	797.4	0.597	0.511
$La_{60}Al_{14}Cu_{26}$	404	679.5	785.6	0.594	0.514
$La_{62}Al_{14}Cu_{24}$	400	681.1	753.4	0.588	0.531
$La_{64}Al_{14}Cu_{22}$	398	682.0	735.6	0.583	0.540
$La_{66}Al_{14}Cu_{20}$	395	681.9	731.0	0.580	0.541
$La_{68}Al_{14}Cu_{18}$	393	682.6	733.2	0.576	0.537
$La_{70}Al_{14}Cu_{16}$	391	682.9	765.5	0.573	0.510
$La_{72}Al_{14}Cu_{14}$	391	682.4	792.7	0.574	0.494
$La_{74}Al_{14}Cu_{12}$	389	681.6	819.6	0.570	0.474
$La_{76}Al_{14}Cu_{10}$	361	675.6	825.5	0.535	0.438

4.2 T_{rg} and glass forming ability

Lu *et al.* have reported that there is a strong correlation between R_c and T_{rg} based on T_g/T_l in many bulk metallic glasses.[8] Figure 4(c) shows the T_{rg} based on T_g/T_l as a function of copper concentration along with the T_{rg} based on T_g/T_m (values are also listed in Table 2). It can be clearly seen from this figure that the T_{rg} based on T_g/T_l exhibits a maximum at $La_{66}Al_{14}Cu_{20}$, while the T_{rg} based on T_g/T_m shows a steady increase with increase in composition. As stated above, $La_{66}Al_{14}Cu_{20}$ has the greatest GFA among these alloys. Therefore, there is a strong correlation between GFA and T_{rg} based on T_g/T_l, not the T_{rg} based on T_g/T_m for the $La_{86-x}Al_{14}Cu_x$ alloys.

5.   Conclusion

A eutectic composition has been found in the $La_{86-x}Al_{14}Cu_x$ ($x = 10$ to 36) alloys, which has the largest GFA in these alloys. It has been found that the best bulk metallic glasses forming alloys are at or near eutectic com-position, a result which is consistent with the fact the reduced glass transition temperature T_{rg} given by T_g/T_l is highest at the eutectic composition. There is a strong correlation between glass forming ability and the T_{rg} based on T_g/T_l in the La-rich La–Al–Cu ternary system.

REFERENCES

1) A. Inoue, T. Nakamura, T. Sugita, T. Zhang and T. Masumoto: Mater. Trans., JIM **34** (1993) 351–358.
2) Z. P. Lu, H. Tan, Y. Li and S. C. Ng: Scripta Mater. **42** (2000) 667–673.
3) Z. P. Lu, Y. Li and S. C. Ng: J. Non-Cryst. Solids **270** (2000) 103–114.
4) A. Inoue, H. Yamaguchi, T. Zhang and T. Masumoto: Mater. Trans., JIM **31** (1990) 104–109.
5) Y. Li, S. C. Ng, C. K. Ong, H. H. Hng and T. T. Goh: Scripta Mater. **36** (1997) 783–787.
6) H. A. Davies: *Rapidly Quenched Metals. Part III*, ed. by B. Cantor, (The Metals Society, London, vol. 1, 1978) pp. 1–21.
7) D. R. Uhlmann and H. Yinnon: *Glasses Science and Technology*, (Academic Press, New York, vol. 1, 1983) pp. 1–47.
8) Z. P. Lu, T. T. Goh, Y. Li and S. C. Ng: Acta Mater. **47** (1999) 2215–2224.